

Turbulent flow drag reduction and degradation with dilute polymer solutions

By R. W. PATERSON† AND F. H. ABERNATHY

Division of Engineering and Applied Physics, Harvard University,
Cambridge, Massachusetts

(Received 28 January 1970 and in revised form 20 April 1970)

Experimental studies of drag reduction and polymer degradation in turbulent pipe flow with dilute water solutions of unfractionated polyethylene oxide are described. Drag reduction results indicate that the magnitude of the reduction cannot be correlated on the basis of weight average molecular weight, rather the phenomenon depends strongly on the concentration of the highest molecular weight species present in the molecular weight distribution. Polymer degradation in turbulent flow is found to be severe for high molecular weight polymers causing appreciable changes in drag reduction and molecular weight with the duration of flow. Data indicates that drag reduction exists in the limit of infinite dilution suggesting that the phenomenon is due to the interaction of individual polymer molecules with the surrounding solvent and that the extent of reduction is relatively independent of pipe diameter when a comparison is carried out at equal solvent wall shear stresses. Consideration of the high viscosity obtained with solutions in an irrotational laminar flow field suggests this is due to polymer molecule deformation and that this phenomenon is central to the mechanism of turbulent flow drag reduction.

1. Introduction

In 1948 Toms reported that very dilute solutions of polymethyl methacrylate in monochlorobenzene could cause large reductions in the turbulent pipe flow pressure drop relative to that obtained with the pure solvent at the same flow-rate (typically a 50 % reduction for a 0.05 % solution). This phenomenon, which has been observed to occur for a number of different polymers and solvents, is commonly referred to as 'drag reduction with dilute polymer solutions' or 'the Toms phenomenon'. While appreciably altering the turbulent flow behaviour, these solutions are observed to cause only a small increase in the laminar flow pipe pressure drop, and hence viscosity, relative to that of the pure solvent.

Since Toms's original studies, the pipe flow experiments of Fabula (1965) and Virk *et al.* (1967) and the rotating coaxial cylinder experiments of Merrill *et al.* (1966) have identified major aspects of the phenomenon such as the dependence of drag reduction on polymer molecular weight, concentration and solvent wall shear stress. The results of other investigators are included in a

† Present address: Fluid Dynamics Laboratory, United Aircraft Research Laboratories, East Hartford, Connecticut.

recent comprehensive review of the subject by Lumley (1969). In general, drag reduction with very dilute solutions is observed to increase with all three variables and significantly, not occur at all for values of the wall shear stress below a certain value. The most effective drag reducing polymers are those with a linear, flexible structure which achieve, on the average, a spherically symmetric distribution of mass elements about the molecule centre of mass, called a random coil, when placed in solution.

While the studies of Fabula, Merrill *et al.* and Virk *et al.* indicated that the turbulent flow field could cause polymer degradation (rupture of polymer molecule valence bonds due to shearing forces resulting in molecular scission) manifesting itself as a decrease in drag reduction effectiveness and polymer molecular weight with time of flow, no studies of turbulent flow degradation have been reported. Since the dependence of drag reduction on polymer molecular weight has been observed to be strong, the present drag reduction study was undertaken with the objective of determining the turbulent shear degradation behaviour in conjunction with the drag reduction behaviour.

2. Experimental procedure

Drag reduction and degradation tests were conducted with dilute water solution of polyethylene oxide ranging in concentration from 0.03 to 75 parts per million (1 p.p.m. = 1 g of dry polymer per 10^6 c.c. of distilled water) and weight average molecular weight from 250,000 to 8,000,000 in both a small (0.248 in. I.D. \times 1700 diameter) and large (0.686 in. I.D. \times 670 diameter) pipe constructed of smooth seamless brass tubing joined in sections by flanges. Each pipe was provided with a pressure drop measuring station near the pipe inlet, station 1, and a second near the pipe exit, station 2, as shown in figures 1 and 2 to permit measurement of the degradation induced change of pressure drop with pipe distance. To obtain a local measurement of the pressure drop, the distance between pipe wall pressure taps at each station was held to 4.5 in. for the small pipe and 36 in. for the large pipe (for Reynolds numbers less than 10,000 a tap separation of 32.5 in. was used in the small pipe to increase signal strength). Figure 1(b) and (c) show pressure tap details for a typical station. Two differential pressure transducers with ranges of 0–1 psi differential pressure were connected to the two stations with the outputs recorded by an integrating digital voltmeter with a 1 sec integration period thereby yielding a steady pressure drop reading.

Degradation measurements were conducted by withdrawing fluid from the test pipes at the three sampling locations shown in figures 1 and 2 and subjecting the samples to intrinsic viscosity measurement to determine solution molecular weight. Samples withdrawn at station 1 and 2 provided local molecular weight measurements which could then be compared to the local pressure measurements at these stations. Samples were withdrawn from the small pipe while turbulent flow took place in the pipe. Since the rate of flow into the sampling lines was about 1/1000 of the pipe flow-rate, the sampling was considered to have a negligible effect on the pipe flow. The low sampling rate and the intense radial mixing by the turbulent flow field produced a sample considered to be representative of the

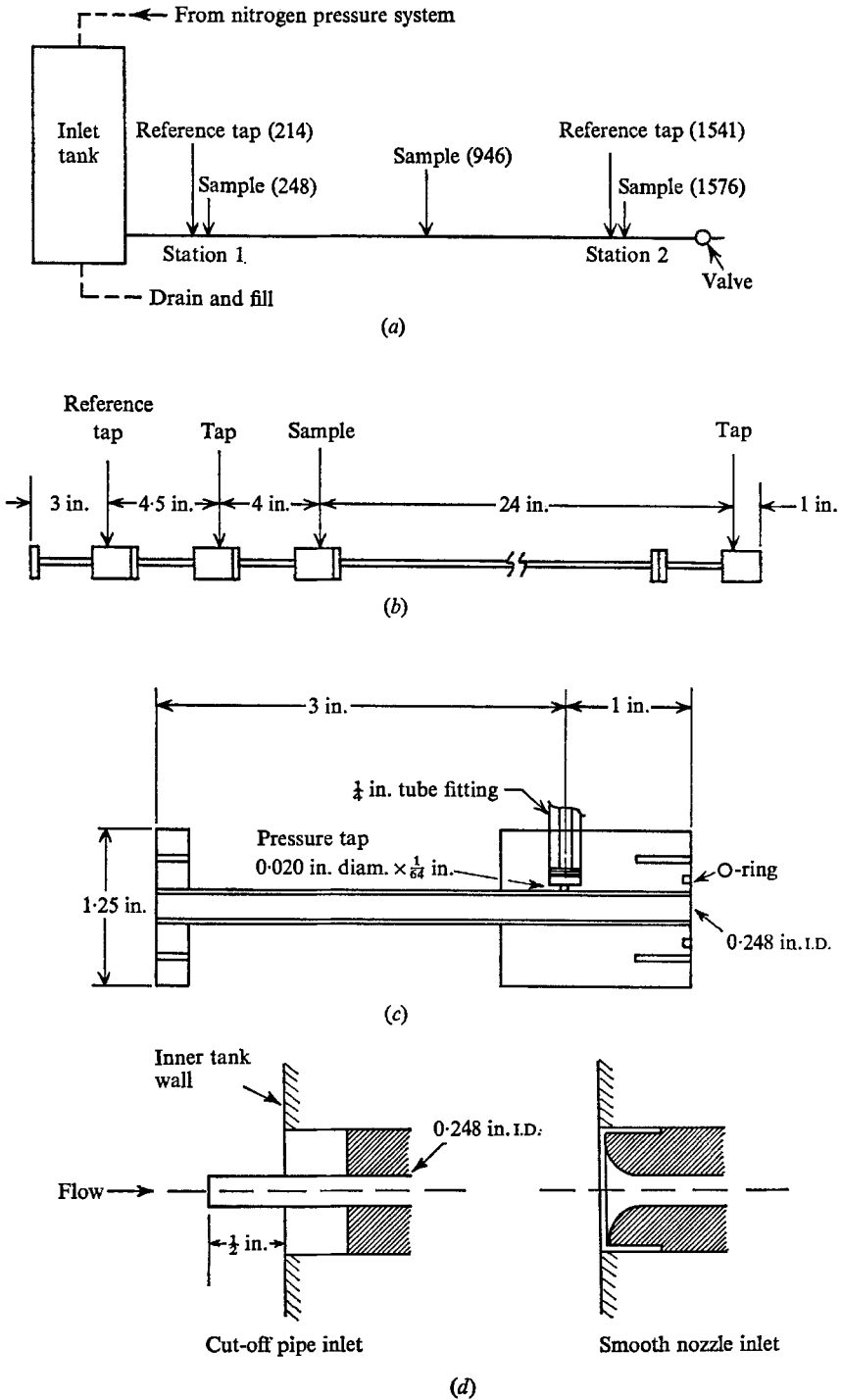


FIGURE 1. 0.248 in. pipe arrangement. (a) Arrangement of pressure and sampling taps. Numbers give distances from pipe inlet to taps in pipe diameters. (b) Detailed station arrangement. (c) Details of typical pressure tap piece. (d) Pipe inlets used with 0.248 in. pipe.

fluid in the pipe at the location of the sampling connexion. Because of the high volume rate of flow in the 0.686 in. pipe and the time required for sample collection, sampling during pipe flow was impractical in this pipe and samples were withdrawn after stopping the flow. Based on the size of the pipe and the volume of fluid withdrawn (150 c.c.), the sample represented an integrated sample over several feet of pipe with the mean location of the sample 25 in. upstream of the

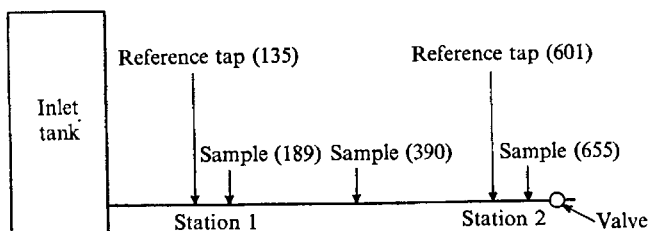


FIGURE 2. 0.686 in. pipe arrangement.

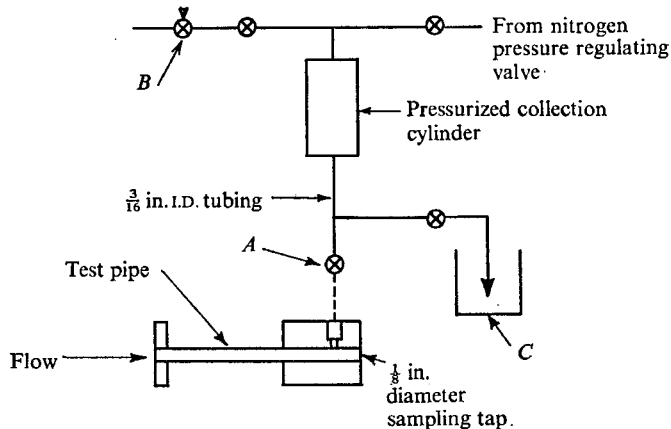


FIGURE 3. Sample collection apparatus. Sampling procedure. (1) Pressurize collection cylinder to local pipe pressure. (2) Open sampling valve *A*. (3) Open pre-set bleed valve *B* to initiate flow into collection cylinder at controlled rate. (4) Depressurize apparatus and collect sample in sample container *C*.

sampling connexion (fluid withdrawn from the pipe was made up by an equal volume of inflow from the inlet tank). The sampling apparatus shown in figure 3 was provided at each sampling location to permit the sample to be collected at a flow-rate below that which causes degradation (wall shear stress in the sampling lines less than 10 dynes/cm²).

The tests were conducted at room temperature (21 to 24 °C) and the mean velocity determined by weighing fluid collected at the pipe outlet over a timed interval. The net accuracy of the velocity and pressure drop measurement was 2% since this was the agreement obtained when distilled water results were compared to the laminar and Blasius smooth pipe turbulent friction factors. Figure 1(*d*) shows the two pipe inlets (smooth nozzle and cut-off pipe inlet) used for the 0.248 in. pipe; only a cut-off pipe inlet was used in the large pipe. To

prevent degradation caused by pumping, a single pass rather than a recirculating system was employed. Pipe flow-rate was controlled by varying nitrogen pressure in the inlet tank and by throttling the pipe outlet valve.

3. Polymer solution preparation

Dilute water solutions of polyethylene oxide, a random coiling linear polymer, were prepared using various molecular weight grades and blends of Polyox, manufactured by Union Carbide Corporation, as shown in table 1. Since a sample of Polyox contains a broad spectrum of molecules of varying molecular weight due to the polymerization process and further blending of batches by the

Polyox grade designation	Manufacturer's blend number	$[\eta]$ (dl/g)	M_w	M_w/M_n	Q
WSR-301	3219	28	8,000,000	—	210
WSR-205	2510	5	1,000,000	20	70
WSR-35	2325	3.0	500,000	14	65
WSR-N750	215	3.5	600,000	7	40
WSR-N80	GM-0242	1.7	250,000	2.5	45

TABLE 1†

† $[\eta]$ measured, M_w calculated from equation (2), M_w/M_n and Q determined by gel permeation chromatography, a process subject to uncertainties as discussed in §4.

manufacturer, the average molecular weight and form of the molecular weight spectrum can be expected to vary amongst samples with the same grade designation but differing manufacturer's blend number. For this reason, quantitative comparison of different drag reduction tests can only be made if the samples are characterized as to molecular weight distribution.

Solutions were prepared by first suspending the dry polymer in a few millilitres of isopropyl alcohol to prevent agglomerate formation and then adding distilled water to yield a solution with a concentration less than 1000 p.p.m. Following solution, this concentrated solution was diluted with distilled water in a mix tank to the desired concentration with the total time between solution preparation and use typically 24 h. Solutions were stirred by hand and transferred from the mix tank to the inlet tank by gravity flow to minimize degradation.

4. Molecular weight measurement

Intrinsic viscosity-molecular weight relation

The parameter relating polymer solution viscosity and molecular weight is the intrinsic viscosity, $[\eta]$, defined as

$$[\eta] = \lim_{\substack{G \rightarrow 0 \\ c \rightarrow 0}} \frac{(n_p/n) - 1}{c}, \quad (1)$$

where n_p is the polymer solution viscosity, n the solvent viscosity at the same temperature, c the polymer concentration and G the shear rate (velocity gradient)

employed in the measurement of n_p . For capillary tube viscometry the value of G evaluated at the tube wall is a convenient measure of the shear rate. The extrapolation of data to zero shear rate is carried out before the extrapolation to zero concentration. Merrill *et al.* (1966) obtained the following intrinsic-viscosity-molecular weight relation for polyethylene oxide in water at 25 °C:

$$[\eta] = (1.03 \times 10^{-4}) \mathbf{M}_w^{0.78}, \quad (2)$$

where the unit for $[\eta]$ is decilitres/gram and \mathbf{M}_w is the polymer solution weight average molecular weight defined as

$$\mathbf{M}_w = \frac{\sum_i N_i M_i^2}{\sum_i N_i M_i}, \quad (3)$$

N_i being the number of molecules of molecular weight M_i . Merrill's viscosity measurements were carried out at wall shear rates less than 20 sec⁻¹ in a Couette viscometer and the weight average molecular weights determined by light scattering. As shown by Flory (1953), equation (2) is only valid if the ratio of weight average to viscosity average molecular weight ($\mathbf{M}_w/\mathbf{M}_v$) is constant for solutions tested. Since degradation would be expected to alter the form of the molecular weight distribution and hence this ratio, the question arises as to the applicability of equation (2) to degraded solutions. The data of Merrill *et al.* show, however, that degraded solutions follow this relation as do both WSR and WSR-N grades of Polyox which have significantly different molecular weight distributions.

Viscosity measurements

Molecular weight measurements were carried out directly on samples of fluid withdrawn from the 0.248 and 0.686 in. pipes by determining the intrinsic viscosity of the solutions at 25 °C and applying equation (2). The viscometer shown in figure 4 was constructed to carry out measurements of the relative viscosity (n_p/n) to high accuracy. In figure 4, the test solution flows from the sample container to a reservoir where the level remains constant by continuously overflowing a small quantity of solution. Flow through the preheat tube raises solution temperature to the water-bath temperature held at 25 °C by a temperature controller. From the preheat tube, the solution enters a second constant level reservoir maintained level by solution overflow, passes through the teflon test capillary tube and enters a third constant level reservoir. Varying the height of the third reservoir varies the gravity driving head and hence the shear rate. Solution overflowing the third reservoir is collected and weighed; the mass flow-rate is determined by the weight collected over an interval timed with a stopwatch, typically 1 h. The ratio of water to polymer solution flow-rate is then the relative viscosity. The flow-rate is below that corresponding to the onset of secondary flow due to tube coiling and the difference between solvent and solution flow-rate is sufficiently small that the kinetic energy correction is negligible. The viscometer operated with a reproducibility of $\pm 0.03\%$ in mass flow-rate measurement which yields an accuracy of $\pm 2\%$ in intrinsic viscosity measurement for a 75 p.p.m. solution with an intrinsic viscosity of 3.0. For solutions of higher intrinsic viscosity, the accuracy is correspondingly higher.

Concentration dependence of solution viscosity

For dilute solutions of random coiling polymers it is experimentally observed (Flory 1953) that the dependence of viscosity on concentration is given by

$$n_p = n(1 + [\eta]c + k[\eta]^2 c^2), \quad (4)$$

where k , the 'Huggins' constant, is approximately constant for a given polymer-solvent system having a value which is usually between 0.35 and 0.40 for viscosity

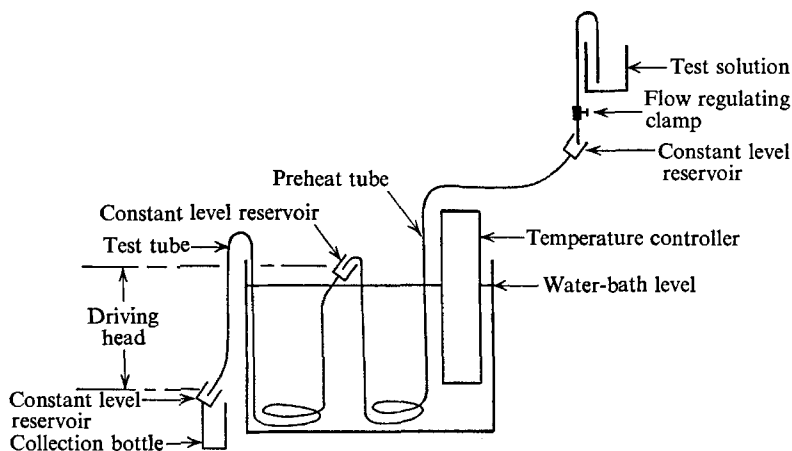


FIGURE 4. Viscometer arrangement. Copper preheat tube of length 10 ft. and 0.065 in. I.D. Teflon test capillary tube of length 18 ft. and 0.034 in. I.D. For tests at wall shear rates less than 50 sec^{-1} , a 50 ft., 0.091 I.D. tube was used to provide a higher flow-rate and thereby increase measurement accuracy.

measurements performed in the limit of zero shear rate. Measurement of the viscosity as a function of concentration for several solutions in the present study yielded a value of 0.4 for k in agreement with values previously reported by Shin (1965). Because concentrations employed in the present study were small (75 p.p.m. or less) experimental extrapolation of the quantity $((n_p/n) - 1)/c$ to zero concentration was not required to determine the intrinsic viscosity. Assuming a value for k of 0.4, the intrinsic viscosity was calculated from equation (4) having measured n_p at small but finite concentration.

Shear rate dependence of solution viscosity

Although previous investigators have reported a negligible dependence of $((n_p/n) - 1)/c$ on shear rate for dilute polyethylene oxide water solutions (Fabula 1966, Virk *et al.* 1967), figure 5 indicates that shear dependence is significant for high molecular weight grades. The effect does not decrease monotonically with decreased average molecular weight, in particular, the degraded WSR-301 solution and the WSR-N750 solution show a small dependence relative to the undegraded WSR grades. Since the variation of this quantity with shear rate should depend strongly on the highest molecular weight components present in the

distribution (Cottrell 1968)†, the data indicates that the degraded WSR solution and WSR-N solution lack the high molecular weight tail present in the undegraded WSR grades. Because of the observed shear rate dependence, viscosity measurements on samples withdrawn from the test pipes were conducted at wall shear rates between 115 and 45 sec⁻¹ and data extrapolated to 15 sec⁻¹ to determine $[\eta]$ (equation (2) is based on measurements at 20 sec⁻¹ or less). It should be noted that this extrapolation is difficult because the rate of change of $[\eta]$ with G is greatest near zero shear.

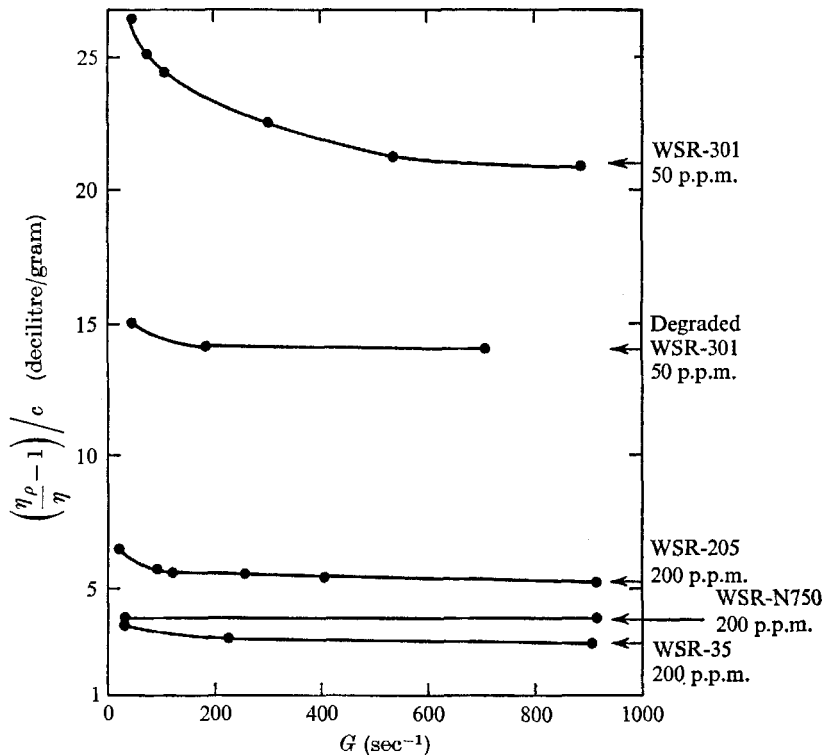


FIGURE 5. Effect of viscometer wall shear rate on the measurement of solution intrinsic viscosity for various dilute polyethylene oxide solutions.

Molecular weight distribution measurements

Because data indicated that the molecular weight dependence of degradation and drag reduction could not be correlated solely on the basis of weight average molecular weight, attempts were made to determine the molecular weight distributions of the various Polyox grades using gel permeation chromatography. Measurements were carried out at 80 °C with a solvent of di-methyl formamide using columns calibrated with narrow fractions of polystyrene. Figure 6 shows distributions determined by this method, the abscissa, A_i , being the chain length of polystyrene molecules used to calibrate the columns. To convert these values to polyethylene oxide molecular weights, the polyethylene oxide molecular weight

† Shear rate behaviour depends on the product M_w .

per unit polystyrene chain length, $Q = M_i/A_i$ must be known. By computing the weight average chain lengths from the distributions ($A_w = \sum_i N_i A_i^2 / \sum_i N_i A_i$) and determining M_w by intrinsic viscosity measurements, the values of $Q = (M_w/A_w)$ shown in table 1 were determined for the various molecular weight grades. Although Q should be a constant amongst the various grades, the variation shown is indicative of severe degradation in the gel permeation chromatography columns, partially due to the high temperature and partially to mechanical shear. The higher value of Q for WSR-35 than WSR-N750 even though WSR-35

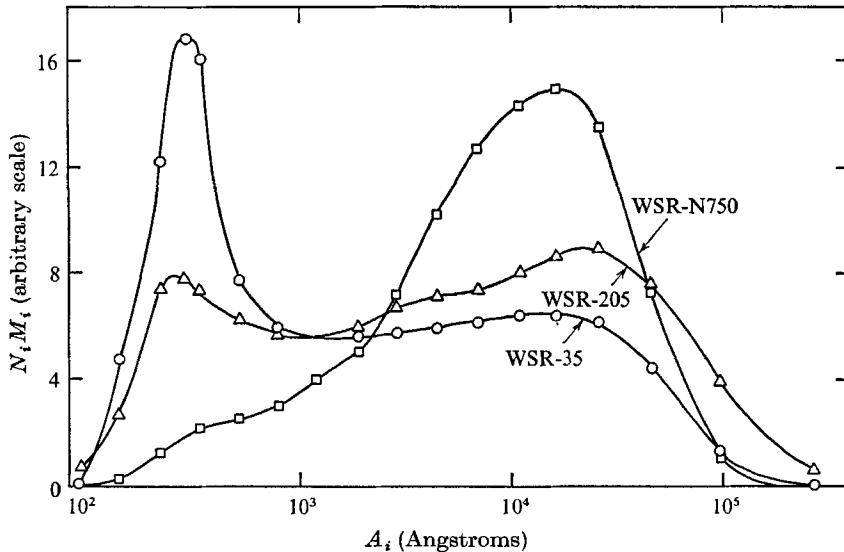


FIGURE 6. Molecular weight distributions for three molecular weight grades of Polyox as determined by gel permeation chromatography. This process is subject to uncertainties as discussed in §4.

has a lower average molecular weight (and therefore should be degraded less) indicates that WSR-35 possesses a high molecular weight tail which has been degraded in the analysis. Table 1 lists values of weight to number average molecular weight ($M_n = \sum_i n_i M_i / \sum_i N_i$) determined from the distribution curves indicating that the WSR-N polymers possess significantly narrower distributions than the WSR polymers; the full magnitude of this difference including the high molecular weight tails present in the WSR polymers has been considerably obscured by degradation. Although these gel permeation results must be considered quantitatively unreliable for reasons cited, it is believed that the above qualitative conclusions are correctly drawn.

5. Effect of degradation on drag reduction

Figure 7 displays pipe friction factor, $f = (2D/\rho V^2)(dp/dx)$, measured simultaneously at stations 1 and 2 in the 0.248 in. pipe as a function of polymer solution Reynolds number ($Re = \rho VD/n_p$) for various concentrations of a low

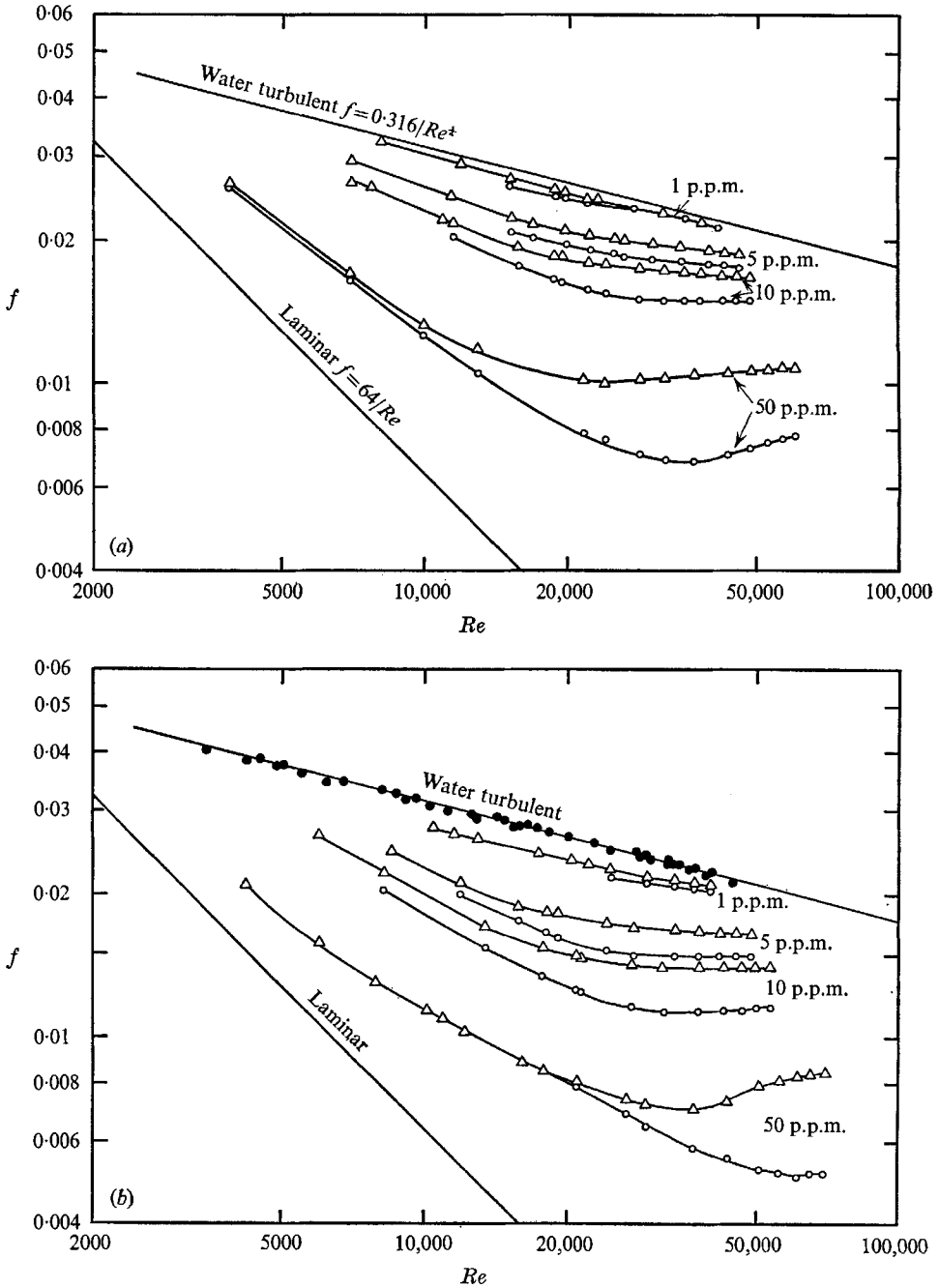


FIGURE 7. Pipe friction factor as a function of Reynolds number for various polyethylene oxide solutions as measured at station 1 (O) and station 2 (Δ) in the 0.248 in. pipe. Inequality of friction factors at the two stations is indicative of polymer degradation during flow. (a) Polymer WSR-35, $M_w = 500,000$ smooth nozzle inlet. (b) Polymer WSR-205, $M_w = 1,000,000$, smooth nozzle inlet. (c) Polymer WSR-301, $M_w = 8,000,000$, cut-off pipe inlet. Turbulent friction factor data for distilled water shown in (b) as solid circles (\bullet).

(WSR-35), moderate (WSR-205) and high (WSR-301) molecular weight polymer. Molecular weights were determined by measuring the intrinsic viscosities of 10 and 50 p.p.m. solutions withdrawn from the inlet tank during testing. Uniform solution preparation procedures produced the same intrinsic viscosities for the 10 and 50 p.p.m. solutions suggesting the quoted molecular weights also apply to the 5 and 1 p.p.m. solutions which were too dilute for meaningful intrinsic viscosity measurement.

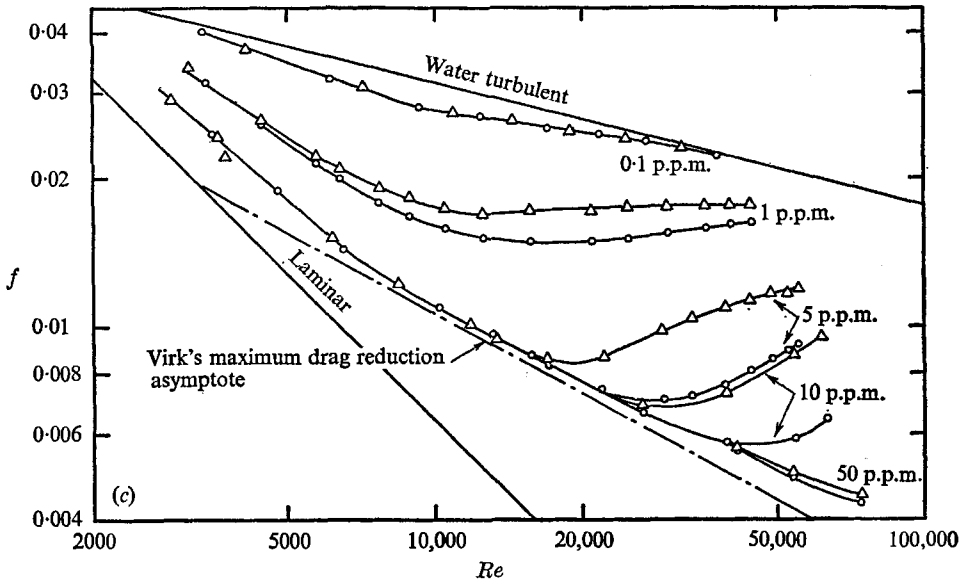


FIGURE 7(c). For legend see previous page.

The low Reynolds number end of the plots represents the point at which transition to turbulence occurred as evidenced by intermittency in the transducer output (alternating patches of laminar and turbulent flow with time). Experience with Newtonian fluids indicates that turbulent pipe flow becomes invariant with pipe distance once the adjacent turbulent patches which occur during transition have merged to form fully developed turbulence. This in conjunction with the fact that concentration is constant indicates that the values of the friction factor at station 2 (triangles) higher than at station 1 (circles) are due to a change in the polymer molecular weight distribution with pipe distance. This change is occasioned by the turbulent flow field itself. The effect is greatest at the higher Reynolds numbers where the stresses tending to rupture the polymer molecule are largest.

Figure 8 compares friction factors obtained with a single polymer solution due to a change of pipe inlet from a smooth nozzle to a high disturbance cut-off pipe inlet. This change appreciably increases the friction factors measured at both stations for the high Reynolds number range where the inequality of friction factors for the smooth nozzle indicated degradation effects were important. The large change in station 1 friction factor suggests that degradation is disproportionately large in the first 200 diameters of flow which precedes

station 1. The high disturbance cut-off pipe inlet shifts the location of turbulent transition toward the inlet thereby increasing the time subjected to turbulence and hence the magnitude of the degradation.

A decrease in drag reducing effectiveness with the high disturbance inlet as compared to the smooth nozzle was generally observed with solutions of WSR-35,

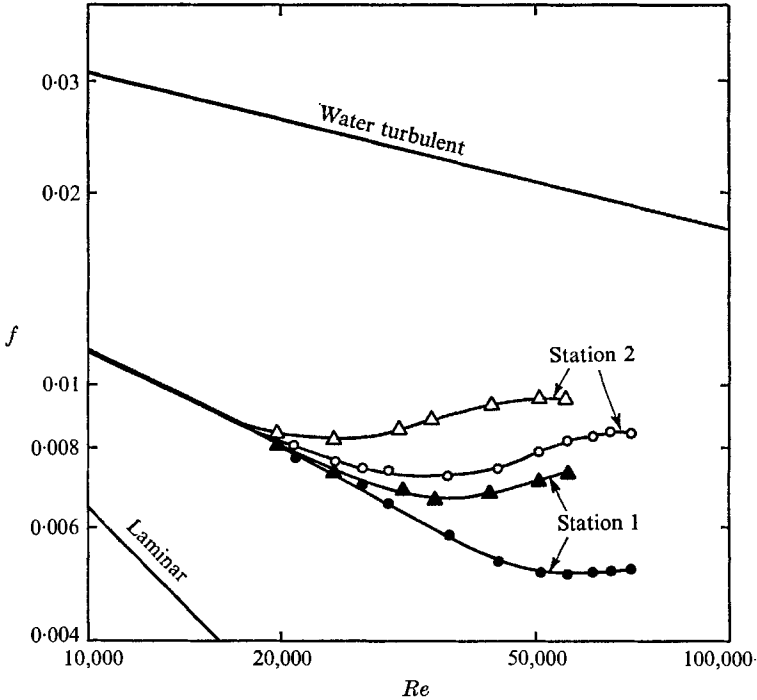


FIGURE 8. Pipe friction factor as a function of Reynolds number for 50 p.p.m. solutions of WSR-205 as measured at stations 1 and 2 in the 0.248 in. pipe showing the effect of a change in the type of pipe inlet from a smooth nozzle (O) to a cut-off pipe inlet (Δ). Curves are identical for Re less than 18,000.

205 and 301 over the concentration range tested (1–75 p.p.m.) in the 0.248 in. pipe. This appreciable change of friction factor with type of inlet and the observed increase with pipe distance means that investigators with different pipe arrangements can obtain friction factors differing by as much as 100% for the same molecular weight solution. This will occur even if the solutions in the inlet tank are characterized as to molecular weight, a procedure which has not been followed in the past.

6. Effect of degradation on polymer solution molecular weight

As evidenced by the friction factor plots given in §5 it is clear that an understanding of the process of shear degradation is essential to the interpretation of drag reduction measurements with high molecular weight polymers. Since polymer solutions can also be degraded by chemical and thermal means, these must also be taken into account when devising handling procedures or carrying

out measurements. For polyethylene oxide in distilled water at room temperature, the chemical and thermal degradation is negligibly small (figure 9) for the times required to withdraw samples from test pipes and carry out molecular weight measurements, thus the primary form of degradation of interest in drag reduction studies is shear degradation.

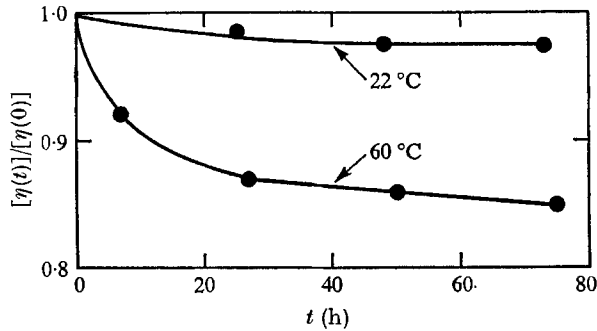


FIGURE 9. Chemical and thermal degradation of a 100 p.p.m. WSR-301 solution as evidenced by a decrease in intrinsic viscosity with time. Time zero corresponds to 24 h after mixing; $[\eta(0)] = 24$.

Shear degradation effects have been noted by a number of investigators. Fabula (1965) noted an increase in turbulent flow pressure drop over the first 400 pipe diameters which he attributed to either molecular disentanglement and/or degradation. In drag reduction studies conducted with coaxial rotating cylinders, Merrill *et al.* (1966) observed that the torque on the inner cylinder increased with time for a fixed rotational speed of the outer cylinder. Merrill attributed this to degradation and extrapolated torque readings to zero time to eliminate the effect of degradation on the measurement. Virk *et al.* (1967) found degradation negligible in tests conducted with a 0.3 cm diameter 'once through' pipe apparatus but severe in a 3.2 cm recirculating apparatus once the wall shear stress exceeded the 'onset wall shear stress'. There have, however, been no studies on the rate of degradation in turbulent flow.

Figure 10 shows degradation of dilute polyethylene oxide solutions as a function of time in the 0.248 in. test pipe for various molecular weight grades. Plotted is the ratio of the intrinsic viscosity measured on samples withdrawn at various pipe locations to the intrinsic viscosity of a sample withdrawn from the inlet tank. The distance from the inlet tank to the sampling station has been converted to a time by use of the measured mean velocity. Shown on each curve is the average wall shear stress experienced by the solution arrived at by averaging the measured pressure drops at stations 1 and 2. This figure demonstrates that the decrease in molecular weight is very rapid in the few tenths of a second required to reach the first sampling station located some 200 diameters from the inlet. The data also indicates, with one exception, that the rate of degradation increases with polymer molecule size (with $[\eta(0)]$) as would be expected since the force tending to rupture the coil will be higher for the larger molecule when subjected to the same shear rate.

Since the wall shear stress for these measurements varied from 210 to 540 dynes/cm² the solutions were not subjected to the same average shear field; however, the differences in the rates of degradation for the various solutions would have been even larger than shown had they been subjected to the same wall shear stress because solutions with the lower degradation rates were tested at higher wall shear stresses. The exception to the statement that the degradation increases with initial polymer solution molecular weight is the solution of

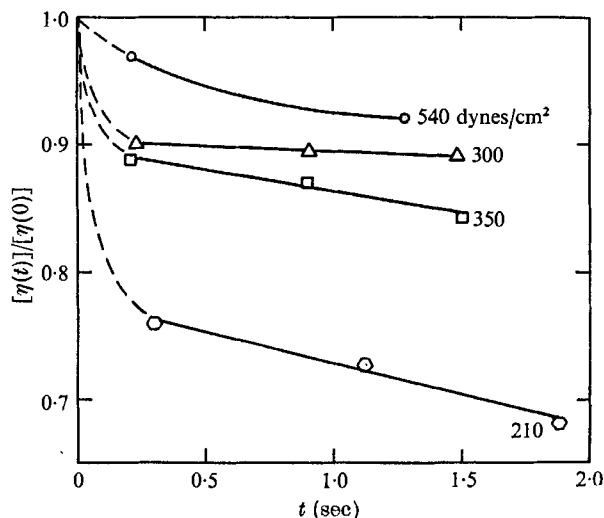


FIGURE 10. Turbulent flow shear degradation of various polyethylene oxide solutions as evidenced by a decrease in intrinsic viscosity with time (pipe distance). Numbers give average wall shear stress experienced by solutions. ○, 50 p.p.m. WSR-301, $[\eta(0)] = 11$, degraded prior to testing; △, 75 p.p.m. WSR-035, $[\eta(0)] = 2.8$; □, 75 p.p.m. WSR-205, $[\eta(0)] = 4.5$; ◇, 50 p.p.m. WSR-301, $[\eta(0)] = 25$. Taken in 0.248 in. pipe equipped with cut-off pipe inlet. Curve unknown in dashed region.

degraded WSR-301 which has a molecular weight five times higher than WSR-35, but a considerable lower rate of degradation (even though the wall shear stress was considerably larger for the degraded WSR-301 solution). The degraded WSR-301 solution was prepared by passing a fresh WSR-301 through the pipe at a Reynolds number of 70,000. This exception demonstrates that the molecular weight dependence of degradation is not uniquely determined by the weight average molecular weight; in particular, it appears that once the high molecular weight components of the molecular weight distribution have been preferentially attacked by the turbulent shear field, the rate of degradation slows down.

To determine the effect of pipe diameter on degradation rate, the ratio of intrinsic viscosity at the various sampling locations to that in the inlet tank was measured in the 0.248 and 0.686 in. pipes at various flow-rates using 50 p.p.m. solutions of WSR-301. As shown in figure 11, the degradation is negligible in both pipes for values of the wall shear stress of 30 dynes/cm² and consistently lower in the larger pipe. It should be noted, however, that while the wall shear stress may be equal in both pipes, the total residence time of a polymer molecule in the intense shear region near the pipe wall, where the majority of the degradation

would be expected to occur, will be smaller for the larger pipe for an equal duration of flow. This arises from the fact that the thickness of the wall region is the same for pipes with the same wall shear stress (as measured in units of the wall length scale $U/[c_w/\rho]^{1/2}$) but the fraction of solution in this region at any time is smaller for the larger pipe.

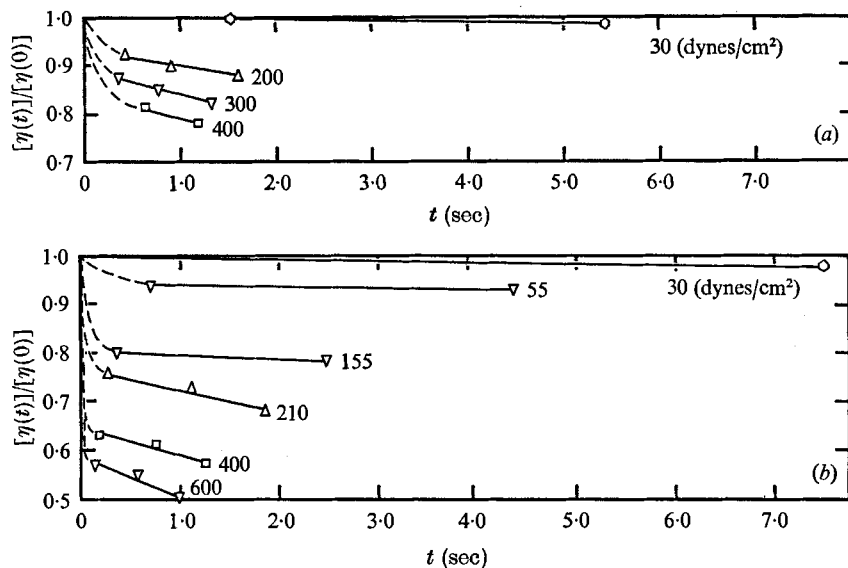


FIGURE 11. Turbulent flow shear degradation of 50 p.p.m. solutions of polyethylene oxide (WSR-301, $[\eta(0)] = 25$) in pipes of differing diameter equipped with cut-off pipe inlets. (a) 0.686 in. I.D. pipe. (b) 0.248 in. I.D. pipe. Curve unknown in dashed region.

These results are in disagreement with those of Virk who found degradation negligible in a small diameter pipe at values of the wall shear stress (above onset) which caused degradation in the larger pipe; these differing results may be due to Virk's use of a pump and recirculating system with the larger pipe.

7. Failure of intrinsic viscosity to correlate the molecular weight dependence of drag reduction

Previous studies have generally shown that the extent of drag reduction increases monotonically with intrinsic viscosity or average molecular weight. An exception to this result is given in the data of Merrill *et al.* where the polymer, WSR-N80 ($[\eta] = 1.8$) showed a several percent higher drag reduction than WSR-N750 ($[\eta] = 3.1$) and WSR-N3000 ($[\eta] = 3.3$). Based on intrinsic viscosity data supplied by the manufacturer, Fabula (1965) also reported this effect.

Figure 12 confirms these results demonstrating that the intrinsic viscosity, in general, fails to correlate the drag reduction for fixed concentration and flowrate. Plotted is an enlarged portion of the friction factor plot in the vicinity of $Re = 45,000$ for 75 p.p.m. solutions of varying molecular weight obtained in the 0.248 in. pipe equipped with a cut-off pipe inlet. The intrinsic viscosities listed

to the right of the data points at $Re = 45,000$ were measured on samples withdrawn from the pipe at the locations of the pressure drop measurement. In general, solutions which have been degraded by virtue of their passage down the pipe (station 2 measurements) show a disproportionately large increase in friction factor for a small decrease in intrinsic viscosity. Since degradation should preferentially attack the highest molecular weight components, the disproportionate decrease in drag reduction with degradation suggests that drag reduction depends primarily on the highest molecular weight species in the distribution.

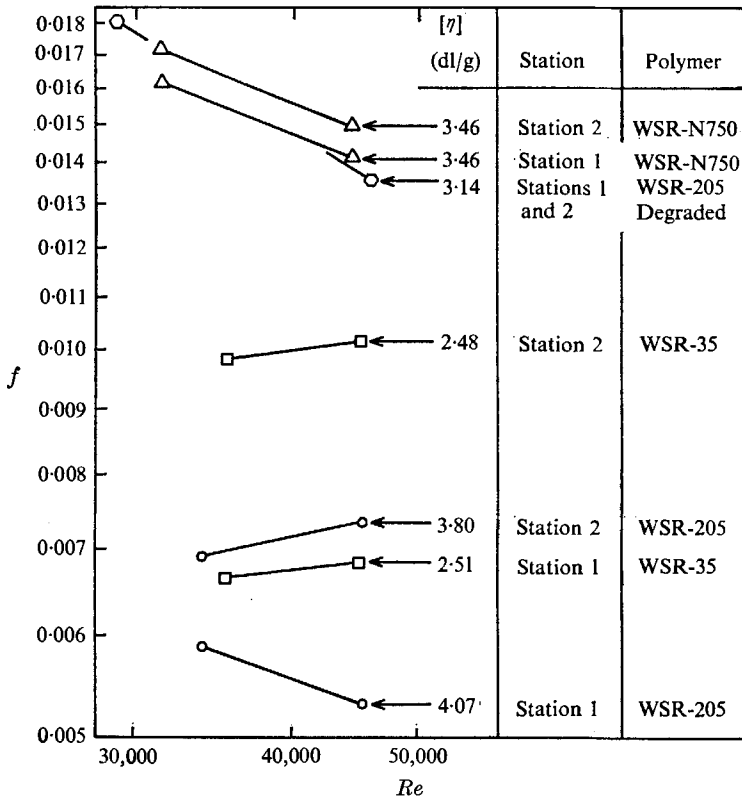


FIGURE 12. Pipe friction factor as a function of Reynolds number for 75 p.p.m. polyethylene oxide solutions showing failure of intrinsic viscosity to correlate the extent of drag reduction.

The failure of the intrinsic viscosity correlation is further seen in comparing data for WSR-N750 and WSR-35 where the former, with an intrinsic viscosity of 3.46 shows twice as large a friction factor as WSR-35 ($[\eta] = 2.51$). This is consistent with the above explanation in that WSR-N750 lacks the high molecular weight tail of WSR-35.

This failure of the intrinsic viscosity to correlate the drag reduction was observed in both pipes and over the range of concentrations and Reynolds numbers considered in this study. A notable example was a 50 p.p.m. solution of WSR-301 which had been degraded in turbulent flow to an intrinsic

viscosity of 10.5 ($M_w = 2,500,000$) and then tested. This solution produced the same friction factor as a 50 p.p.m. WSR-205 solution of intrinsic viscosity 3.6 ($M_w = 650,000$) at a Reynolds number of 50,000 in the 0.248 in. pipe. Additional examples of this effect are detailed elsewhere (Paterson 1969).

These results indicate that the weight average molecular weight may have little relevance to the actual drag reduction behaviour. Unless tests are conducted on narrow molecular weight fractions and the shear rate is sufficiently low that degradation does not cause significant shifting and broadening of the distribution, there is little possibility that the true dependence of drag reduction on concentration and molecular weight will be established. For polyethylene oxide, data on the WSR-N grades is more valid than data on the WSR grades since the distribution is narrower and the degradation rate is less.

8. Onset of drag reduction and Virk's hypothesis

Based on tests with water solutions of polyethylene oxide and the results of other investigators with different polymer-solvent systems, Virk *et al.* (1967) showed that dilute polymer solutions produce no drag reduction until the wall shear stress is increased to the point at which the following relation between the turbulence wall length scale and the radius of gyration of the polymer molecule in solution, R_g , is satisfied:

$$2R_g/(U/[c_w/\rho]^{1/2}) = 0.015 \pm 0.005 = \text{onset constant.} \quad (5)$$

Virk found the point of onset of drag reduction to be independent of polymer concentration over the range from about 10 to several thousand p.p.m. and independent of pipe diameter.

Figure 13 shows the onset of drag reduction in the present study for various concentrations of WSR-301 taken in the 0.686 in. pipe. The point of onset is seen to move to higher Reynolds numbers and hence higher values of wall shear stress as the concentration decreases. Table 2 summarizes onset constants obtained in the present study for various solutions in both pipes. The radius of gyration was obtained from intrinsic viscosities measured on solutions withdrawn from the pipes at the onset point and conversion of these values to radii of gyration using the 'z average' radius of gyration-intrinsic viscosity relation of Merrill *et al.* (1966).

Although the data shows a dependence on concentration and a variation in the onset constant in excess of that reported by Virk, the present tests are considered to generally confirm Virk's onset criterion. Tests on monodisperse samples are required to establish whether the variation in onset constant amongst various molecular weight grades is due to the polydispersity of the samples; the good agreement obtained with the degraded WSR-205 solution which had been narrowed by the degradation process indicates polydispersity may account for some of the variation. The tests indicate a dependence on concentration as intuition might suggest; however, this dependence is considerably weaker than the dependence on radius of gyration.

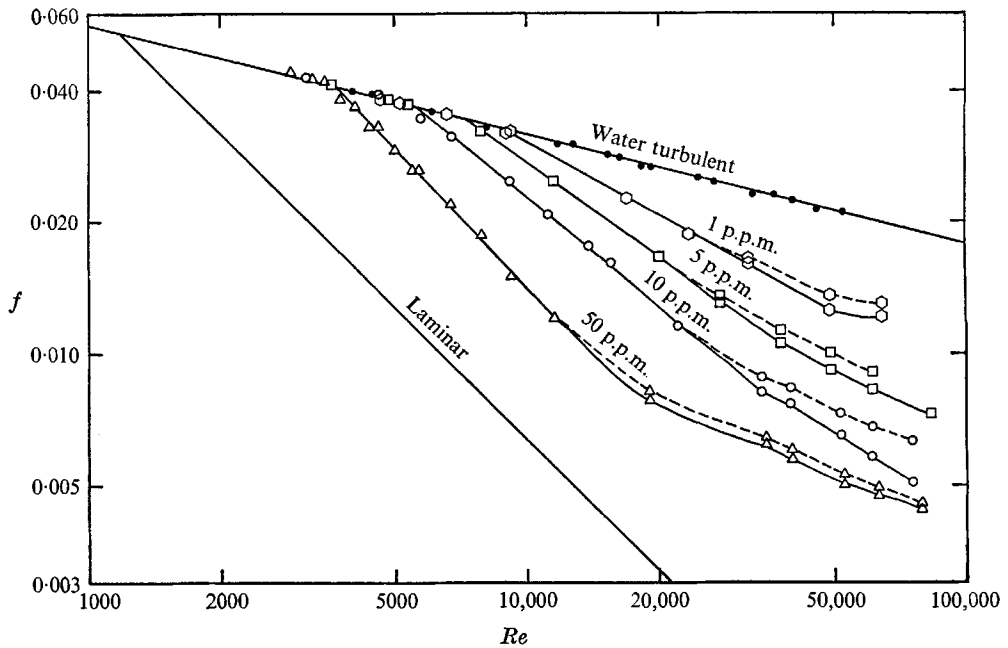


FIGURE 13. Pipe friction factor as a function of Reynolds number for polyethylene oxide (WSR-301) solutions of varying concentration in the 0.686 in. i.d. pipe showing a variation in the Reynolds number for the onset of drag reduction with polymer concentration. Dashed lines show deviation of station 2 measurements from station 1 measurements at high Reynolds number due to degradation. Distilled water data shown as solid circles.

Pipe (in.)	Polymer	Concentration (p.p.m.)	(dl/g)	Onset constant
0.686	WSR-301	1	28†	0.021
0.686	WSR-301	5	28†	0.018
0.686	WSR-301	10	27	0.013
0.686	WSR-301	50	28	0.009
0.686	WSR-205	1	5.5†	0.010
0.686	WSR-205	10	5.5	0.007
0.686	WSR-205	50	5.2	0.006
0.686	WSR-35	1	3.0†	0.008
0.686	WSR-35	10	3.0	0.005
0.686	WSR-35	50	3.2	0.005
0.686	WSR-N750	50	3.8	0.011
0.248	WSR-N750	75	3.5	0.013
0.248	WSR-205	75	3.1	0.017

TABLE 2

† For table entries denoted by a dagger, the low concentrations precluded intrinsic viscosity measurements and the value for $[\eta]$ was assumed equal to that measured on the more concentrated solutions of the same molecular weight grade.

9. Dependence of drag reduction on concentration

Figure 7(c) is a friction factor plot for a high molecular weight polymer obtained in the 0.248 in. pipe equipped with a cut-off pipe inlet. This figure displays saturation in which a concentration is reached above which further increases produce no further drag reduction but serve only to increase the viscosity. This effect was reported by Virk and his 'maximum drag reduction asymptote', which was found to define the saturation limit for polyethylene oxide solutions in both a 0.292 cm and 3.21 cm pipe, is plotted in figure 7. The agreement with Virk's asymptote is good except at high Reynolds numbers where degradation effects become important. A comparison of parts (a), (b) and (c) of figure 7 demonstrates that the concentration required for saturation decreases with increased average molecular weight, thus WSR-205 saturates between 10 and 50 p.p.m. and WSR-301 saturates between 1 and 5 p.p.m. Using the intrinsic viscosity-radius of gyration relationship of Merrill *et al.* (1966), these concentrations are found to correspond to a ratio of polymer molecule centre-to-centre separation to polymer coil diameter of about 2 or 3. In this condition, neighbouring polymer coils are almost in direct contact with one another.

Figure 7(c) indicates that solutions of higher concentration require higher flow-rates before degradation effects become noticeable. This can be explained if one assumes that the drag reduction depends primarily on the concentration of the high molecular weight components. Above a certain concentration of these components, the solution is saturated. As degradation attacks the higher components, the weight average molecular weight decreases but the drag reduction remains unaltered as long as the concentration is above saturation. This indicates that friction factor data is an unreliable indicator of degradation; whereas figure 11 shows appreciable degradation for 50 p.p.m. WSR-301 at a wall shear stress of 210 based on molecular weight measurements, the friction factors at stations 1 and 2 are equal in figure 7(c) at $Re = 36,000$, the value of Reynolds number corresponding to this wall shear stress.

If the phenomenon of drag reduction is due to the interaction of isolated polymer molecules with the surrounding solvent rather than on interparticle effects, the drag reduction would be expected to increase linearly with concentration at least for low concentrations. In particular, the parameter D defined as

$$D = f_p/f, \quad (6)$$

where f_p and f are the polymer and solvent turbulent pipe friction factors, respectively, measured at the same Reynolds number in a given pipe, would be expected to depend on concentration as follows:

$$D = 1 - dc, \quad (7)$$

where ' d ' is the limit of the quantity $-(D-1)/c$ at zero concentration. The quantity ' d ' gives the drag reduction obtained when the first polymer molecule is introduced into the solvent and would be expected to depend on the polymer molecular weight and the flow variables. Figure 14 is a plot of the function $-(D-1)/c$ versus concentration for three molecular weight grades taken at a

Reynolds number of 10,000 in the 0.248 in. pipe. The trend toward zero slope at low concentrations appears to confirm a linear dependence on concentration. Unless the plot goes to zero for concentrations approaching zero, drag reduction exists in the limit of infinite dilution. Although such a plot requires only measurement of relative friction factors of solvent and solution, large errors can result in the calculated value of 'd' when the friction factors approach equality. Experiments designed to measure the extent of drag reduction to high precision are needed to establish firmly the low concentration drag reduction behaviour of polymer solutions.

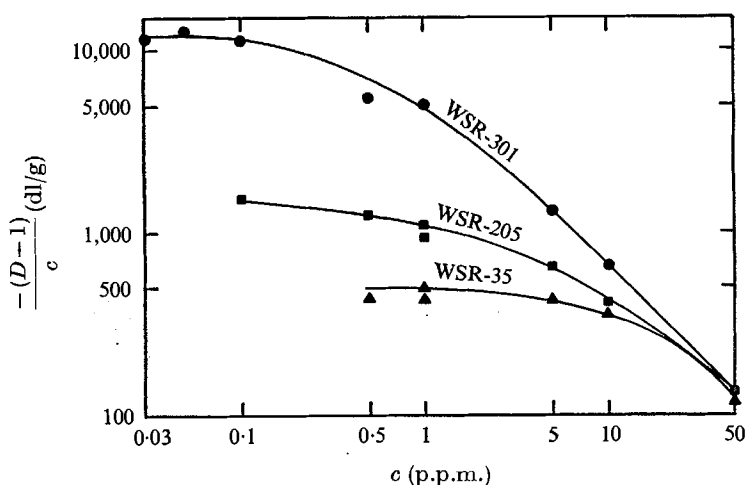


FIGURE 14. Drag reduction per unit concentration as a function of concentration obtained in the 0.248 in. pipe at $Re = 10,000$.

10. Theoretical explanations for drag reduction

Since the friction factors for turbulent pipe flow of Newtonian fluids are not currently calculable from the Navier–Stokes equation, a ‘theory’ for turbulent flow drag reduction, where the constitutive relation and hence equation of motion is unknown, must necessarily be limited. Representative of existing theories are the aggregation theory of Fabula, Lumley & Taylor (1966), the anisotropic viscosity theory of Merrill *et al.* (1966) and the visco-elasticity theory of Walsh (1967). Recently, Lumley (1969) has pointed to the possible connexion between drag reduction and the behaviour of dilute polymer solutions in irrotational laminar flow fields. Whereas the viscosity of these solutions is only slightly greater than the pure solvent (1.125 times that of water for 50 p.p.m. WSR-301) when measured in the rotational Couette or Poiseuille flows, a drop of solution, such as 50 p.p.m. WSR-301, pulls out into a long thread when it falls from a stirring rod. A column of solution falling from a beaker resembles glycerin in that the column pulls out into a long thread rather than breaking up into drops at intervals on the order of the column circumference. Measurement of the solution surface tension yields values essentially the same as those of the pure solvent.

The behaviour correlates with drag reduction results in that 100-fold higher concentrations are required to observe the effect with WSR-N than WSR grade polyethylene oxide.

This apparent difference in viscosity between rotational and irrotational flow fields is believed to be related to the fact that the forces tending to deform the spherical polymer coil in an irrotational flow field are unidirectional; the resultant deformation of the coil is expected to be large, much as in the case with Taylor's (1934) 'hyperbolic' flow field studies with liquid drops immersed in a second liquid. Dissipation within the coil during deformation in addition to the work required for elastic deformation would be expected to contribute to a high solution viscosity. Direct calculation of this effect appears difficult and to quote Taylor (1932) for the simpler problem of the viscosity contribution of a deformable drop, "the difficulties in the way of a complete theory when solid particles are replaced by fluid drops are almost insuperable".

The fact that turbulent flow drag reduction and the high solution viscosity in an irrotational flow field are the only two large macroscopic effects observed with minute concentrations suggests the two phenomena are related. Lumley (1969) has noted that the presence of such irrotational flow fields near the wall has been suggested by the work of Kline *et al.* (1967). Such a high viscosity would be expected to oppose the intensification of vortices near the wall and hence decrease the rate of 'bursting'.

Such an explanation is based on the interaction of a single polymer molecule with surrounding solvent and therefore indicates that drag reduction should exist in the limit of infinite dilution as appears to be the case. It is based on a laminar flow property of dilute solutions which is consistent with the fact that the turbulent flow field should appear to the minute molecule as a laminar flow. It avoids the difficulty of comparing polymer length scales and turbulent eddy length scales (some two orders of magnitude larger as evidenced by the value for the onset constant) since it depends on a continuum property of the fluid in a particular straining field rather than on the direct geometrical interference between a polymer molecule and an eddy. Finally, the deformation and hence viscosity contribution would be expected to depend on the strain rate near the wall and on the concentrations of the largest molecules present in the distribution, as appears to be the case with drag reduction.

11. Conclusions

The experimental studies reported here indicate that the use of fractionated polymer solutions in flow situations where degradation is either negligible or taken into account is critical to the determination of the concentration and molecular weight dependence of drag reduction. Measurements of this nature are required to obtain a body of data to which the non-dimensional parameters arising from theory may be compared; such data is not presently available. The need for measurements of polymer solution viscosity in irrotational flow fields and correlation of these results with a mathematical model of polymer deformation is also indicated.

This study was supported in part by the Office of Naval Research under Contract N00014-67-A-0298-0002, and by the Division of Engineering and Applied Physics, Harvard University.

REFERENCES

- COTTRELL, F. R. 1968 An experimental study of the conformation of Polyisobutylene in hydrodynamic shear field. Sc.D. Thesis, M.I.T.
- FABULA, A. G. 1965 The Toms phenomenon in the turbulent flow of very dilute polymer solutions. *Proc. 4th Int. Congress on Rheology, Part 3*, pp. 455-479. Interscience.
- FABULA, A. G. 1966 An experimental study of grid turbulence in dilute high-polymer solutions. Report to U.S. Bureau of Naval Weapons via Office of Naval Research.
- FABULA, A. G., LUMLEY, J. L. & TAYLOR, W. D. 1966 Some interpretations of the Toms effect. In *Modern Developments in the Mechanics of Continua*. Academic.
- FLORY, P. J. 1953 *Principles of Polymer Chemistry*. Cornell University Press.
- KLINE, S. J., REYNOLDS, W. D., SCHRAUB, F. A. & RUNSTADLER, P. W. 1967 *J. Fluid Mech.* **30**, 741-73.
- LUMLEY, J. L. 1969 *Annual Review of Fluid Mechanics*. Palo Alto, California: Annual Reviews, Inc.
- MERRILL, E. W., SMITH, K. A., SHIN, H. & MICKLEY, H. S. 1966 Study of turbulent flows of dilute polymer solutions in a Couette viscometer. *Trans. Soc. Rheology*, **10**, 335-351.
- PATERSON, R. W. 1969 Turbulent flow drag reduction and degradation with dilute polymer solutions. *Office of Naval Research, Contract N00014-67-A-0298-0002*.
- SHIN, H. 1965 Reduction of drag in turbulence by dilute polymer solutions. Sc.D. Thesis, M.I.T., Cambridge, Mass.
- TAYLOR, G. I. 1932 The viscosity of a fluid containing small drops of another fluid. *Proc. Roy. Soc. A* **138**.
- TAYLOR, G. I. 1934 The formation of emulsions in definable fields of flow. *Proc. Roy. Soc. A* **146**, 501.
- TOMS, B. A. 1948 Some observations on the flow of linear polymer solutions through straight tubes at large Reynolds numbers. *Proc. 1st Int. Congress on Rheology*, vol. II, pp. 135-41. North Holland.
- VIRK, P. S., MERRILL, E. W., MICKLEY, H. S., SMITH, K. A. & MOLLO-CHRISTENSEN, E. L. 1967 The Toms phenomenon: turbulent pipe flow of dilute polymer solutions. *J. Fluid Mech.* **30**, 305-28.
- WALSH, M., 1967 On the turbulent flow of dilute polymer solutions. Ph.D. Thesis, Cal. Inst. Tech., Pasadena, California.